THE DEVELOPMENT AND USE OF ENVIRONMENTALLY-ASSISTED CRACKING MODELS FOR LIGHT WATER REACTORS

F.P. FORD

General Electric Corporate Research and Development Center
1 River Road, Schenectady, New York 12301, USA

ABSTRACT

The objective of this paper is to detail the logical development of mechanistically-based models of environmentally-assisted crack initiation and growth for stainless and low-alloy steels and nickel-base alloys used in Boiling Water Reactors and to show how these models are being used to predict, and thereby define mitigating actions for cracking in stainless steel piping and core components, nickel-base alloys and low alloy steel pressure vessels.

INTRODUCTION

Crack initiation and propagation in structural materials due to stress corrosion, corrosion fatigue or hydrogen embrittlement continue to pose economic and potential safety problems in, for instance, the power generation, chemical, petrochemical and aerospace industries. The reason for this lies in three factors. First, as design lives increase, so the quantitative definition of cracking susceptibility changes; for instance, the extremely low crack propagation rate of stainless steel in ultra high purity water would, in previous times, have been regarded as "zero" cracking susceptibility, but these rates can be of potential significance for design lives > 40 years. Thus, the number of material/environment/stress systems which show relevant cracking susceptibilities is forever increasing. Second, the current life prediction codes are based either on a relatively scattered data base, or do not account for the wide range of material/environment conditions that can exist in an operating plant. Thus, there is no guarantee that the predicted life according to these codes necessarily applies to the specific component under consideration. Third, the mechanistic understanding of the cracking process has tended to be qualitative, and this has made it hard to predict the sensitivity of cracking susceptibility to subtle changes in the myriad of material, environment and stress parameters that are conjointly required for environmentally-assisted cracking to occur. Thus, it is not surprising that environmentally-assisted cracking in operating plant has gained the reputation of being non-reproducible or non-predictable.

The objective of this paper is to address the third of the above items and to illustrate how recent advances in our mechanistic understanding of environmentally-assisted cracking may be used for practical design and system operating purposes.

THE PROBLEM OF SYSTEM DEFINITION

In order to derive a deterministic model of cracking, it is necessary to define the steady-state and transient environment, material and stressing conditions that exist for a specific component. Any uncertainty in this system definition will automatically lead to a corresponding scatter in the predicted cracking response. This scatter is illustrated schematically in Figure 1 by the "upper" and "lower" a_t values, which correspond quantitatively to the "worst" and "best" conceived combinations of the relevant system conditions. Thus, for the purpose of this paper, it is assumed that an adequate system definition is possible.

A further problem of definition occurs in differentiating between crack initiation and propagation. To a certain extent this division is arbitrary since it will depend on the sensitivity of crack detection or crack following. For the purpose of model development, it is assumed that environmentally-assisted cracking starts at localized corrosion or mechanical defect sites; such sites are associated with for instance, pitting, intergranular attack, scratches or weld defects. If it is further assumed that the probability of such initiation sites existing relatively early in the life of the component is high, then the problem of life-prediction narrows down to understanding the growth of small cracks from each of these geometrically-separated initiation sites, and the coalescence of these small cracks to form a major crack which may then accelerate or arrest depending on the specific material, environment and stress conditions. There has been relatively little fundamental work on the growth of such microscopically short cracks. For sake of brevity, this will not be reviewed in detail, apart from mentioning that most work has been done under fatigue loading [1-5], with emphasis on the microstructural interactions required for microscopic crack arrest or propagation, and how linear elastic fracture mechanics analyses have to be modified in this crack size range. In the area of environmentally-assisted cracking, the coalescence of microscopically small cracks has been investigated for carbon steels (in carbonate/bicarbonate solutions)[6,7] and stainless steels and nickel-base alloys[8] in high temperature water. In these cases it is observed that the crack growth rate increases as the small cracks coalesce, and approaches a steady-state value when the mean crack depth is of the order of 50 μm (Figure 2), and where the crack propagation rate may be analyzed in terms of linear elastic fracture mechanics normally applicable to "long" cracks.

Thus, mechanistic knowledge of propagation rates of "long" cracks may be used for life prediction, recognizing that the resultant lives may be conservative because the crack initiation at pits, etc. and subsequent crack coalescence periods are not taken into account.

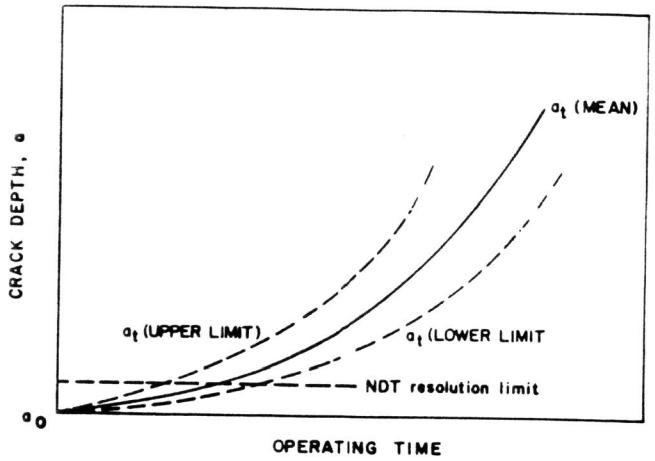

Figure 1. Schematic variation of crack length with time due to environmentally-assisted cracking showing the curves for the mean system conditions, and the limiting values associated with extremes in material, environment and stressing conditions.

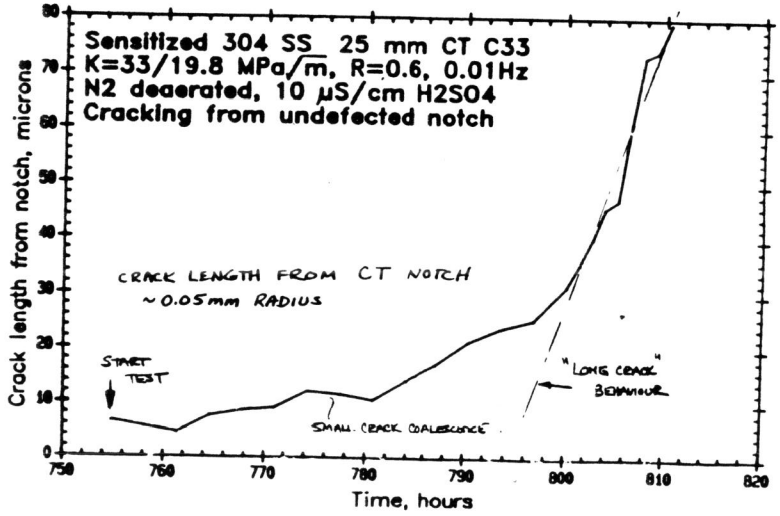

Figure 2. Crack depth/time relationships observed during early crack growth/coalescence in the stainless steel/288°C water system. (8)

CANDIDATE CRACK PROPAGATION MODELS

The basic premise for all of the proposed crack propagation mechanisms for ductile alloys in aqueous solutions is that the crack tip must propagate faster than the corrosion rate on the unstrained crack sides; if this were not the case, the crack would degrade into a blunt notch[9,10]. Based on this rather obvious criterion, the material/environment conditions for cracking to be possible may be defined based on the thermodynamic criteria for the existence of a protective oxide, salt or compound film on the crack sides. For instance, the well known cracking susceptibility of mild steel in hydroxide, carbonate/bicarbonate, nitrate, phosphate and molybdate-containing solutions may be predicted to occur in the specific potential/pH ranges where the protective film is thermodynamically stable [11]. Very similar thermodynamic arguments may be made for other systems, (e.g. brass/ammoniacal solutions [12]), and may be extended to kinetic arguments [13-15] that the electrochemical reaction rates (e.g. dissolution or oxidation) at the strained crack tip must be significantly higher than those on the crack sides for an "electrochemical knife"[13] to propagate. Indeed the suppression of both stress corrosion and corrosion fatigue in many systems may be explained in terms of blunting of cracks during the early propagation stage. The cracking of mild steel and low-alloy steels in aqueous environments offer ideal examples of this criterion. For instance, low-alloy steels will not exhibit stress corrosion in acidic or concentrated chloride solutions unless the general corrosion/blunting effect is counteracted with chromium or nickel alloying additions [11,16]. Similar blunting explanations may be proposed for the relative ease of corrosion fatigue crack initiation of aluminum in chlorides in comparison to hydroxides [17], etc.

Provided there is a mechanism for preventing chemical blunting of the crack, numerous crack propagation mechanisms were proposed in the period 1965-1979 [18-28], ranging from the pre-existing active path mechanisms, through the strain-assisted active path mechanisms to those depending on various absorption/absorption phenomena (e.g., hydrogen embrittlement mechanisms). There was considerable debate concerning the dominant mechanism in a given system, promulgated in part by the fact that up to 15 years ago there were few analytical techniques to test quantitatively the various hypotheses. Parkins [29] pointed out early on, however, that it was likely that there was a "stress corrosion spectrum" which logically graded the cracking systems between those that were mechanically dominated, (for instance, hydrogen embrittlement of high strength steels), to those that were environmentally dominated (for instance, pre-existing active path attack in the carbon steel/nitrate system). Indeed, it was suggested that two mechanisms may operate in one alloy/environment system with a dominant mode being determined by relatively small changes in the material, environment or stressing conditions. This rationalization was followed by the suggestion (e.g., 9, 30-32) that a similar spectrum of behavior occurs between constant load (stress corrosion), dynamic load (strain-induced cracking), and cyclic load (corrosion fatigue) conditions.

With the advent in the last 15 years of more sensitive analytical capabilities, many of the earlier cracking hypotheses have been shown to be untenable, and the candidate mechanisms for environmentally-assisted crack propagation (for both stress corrosion and corrosion fatigue) have narrowed down to slip dissolution, film-induced cleavage and hydrogen embrittlement.

In order to restrict further discussion. attention is focused on ductile alloys in high temperature water symptomatic of Light Water Reactor operations. Of the various crack propagation models mentioned above, the slip-dissolution mechanism will be used as the working hypothesis.

MODEL FORMULATION AND QUANTIFICATION

The slip dissolution/film rupture mechanism of environmentally assisted cracking relates crack advance to dissolution reactions at the crack tip where a thermodynamically stable oxide is ruptured by increasing strain in the underlying matrix. The periodicity of this film rupture event is related to the strain rate in the metal matrix and this, in turn, is controlled by either creep processes under constant load or applied strain rates under monotonically increasing or cyclic load conditions. Thus, the model is potentially applicable not only to stress corrosion (under constant stress) but also to corrosion fatigue over the range of stress amplitude, mean stress, frequency, etc. combinations.

The change in oxidation charge density with time following the rupture of a protective film at the crack tip is shown schematically in Figure 3. This oxidation is due to a mixture of the dissolution of the exposed metal matrix, and oxide nucleation and growth; in either case the original metal interface is being transformed i.e. the crack tip is advancing. The amount of metal transformed to dissolved species or oxide, may be related faradaically to the total oxidation charge density. Since a protective oxide thermodynamically wants to reform at the bared surface, the rate of oxidation or crack tip advance will slow with time because of this passivation effect. Thus, crack advance can only be maintained if the film rupture process reoccurs. Therefore, for a given crack tip environment, potential and material condition, the crack propagation rate will be controlled by both the change in oxidation charge density with time and the frequency of film rupture at the strained crack tip. This latter parameter will be determined by the fracture strain of the film, ε_f, and the strain rate at the crack tip, $\dot{\varepsilon}_f$. Therefore, by invoking Faraday's law, the average environmentally-controlled crack propagation rate, $\bar{v}_t$, is related to the oxidation charge density passed between film rupture events, Q_f, and the strain rate at the crack tip.

$$\bar{V} = \frac{M}{zpF} \cdot \frac{Qf}{\varepsilon_f} \cdot \dot{\varepsilon}_{ct} \qquad [1]$$

where

M, p = atomic weight and density of the crack tip metal

F = Faraday's constant

z = number of electrons involved in the overall oxidation of an atom of metal

Because the oxidation charge density on a bare surface varies with time at a rate that is dependent on the material and environment compositions at the crack tip, it follows that Equation 1 may be reformulated in terms of a more general power law relationship:

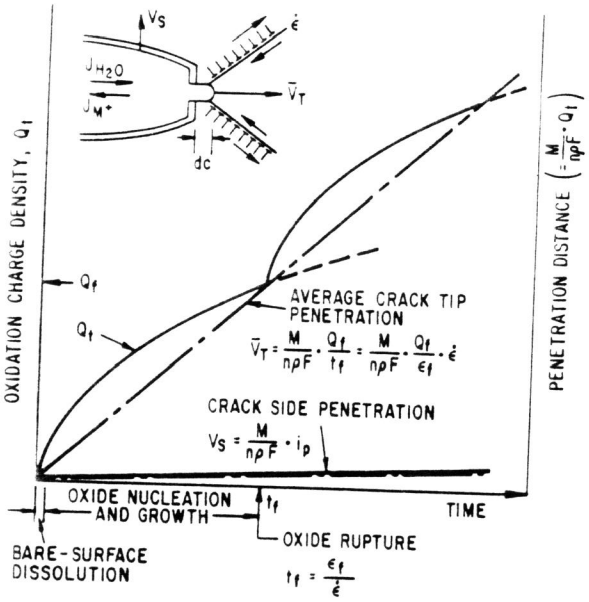

Figure 3 Schematic oxidation charge density/time relationship for a strained crack tip and unstrained crack sides.

$$\bar{V}_t = A\dot{\epsilon}_{ct}^{n} \qquad [2]$$

where A and n are constants, depending on the material and environment compositions at the crack tip. These constants may be related quite specifically to details of the oxidation reactions at the crack tip. This is illustrated in Figure 4 by the oxidation current density/time transients which occur when the protective oxide is ruptured. These transients generally have an initially high bare surface dissolution current density, i_o, that may exist for a time t_o. After this time, oxide formation or precipitation leads to a decay in the oxidation current density, given by a general relationship;

$$i_t = i_o\left(\frac{t}{t_o}\right)^{-n} \qquad [3]$$

If the bare surface condition is maintained at the crack tip, i.e., when $\epsilon_{f/\dot{\epsilon}_{ct}} \leq t_o$, (where ϵ_f = fracture strain of oxide and $\dot{\epsilon}_{ct}$ = crack tip strain rate), then integration of Equation 3 leads to a predicted maximum crack propagation rate:

$$\bar{V}_{max} = \frac{M}{zpF} i_o \qquad [4]$$

This relationship is the quantitative basis for the early empirical observations shown in Figure 5 for various alloy systems in relatively concentrated environments.

In recent years the emphasis has been on studying cracking in dilute environments and constant load conditions where the relevant crack propagation rates are $< 10^{-7}$ cms^{-1}. Under these circumstances a bare surface is not necessarily maintained at the crack tip, and the crack propagation rate is defined by:

$$\bar{V}_{max} = \frac{M}{zpF}\frac{i_o t_o^{n}}{(1-n)\epsilon_f^{n}}\cdot\dot{\epsilon}_{ct}^{n} \qquad [5]$$

where the parameters relate to the bare surface oxidation kinetics (i_o, t_o, n) shown schematically in Figure 4.

One limit to the validity of this relationship (equation 5) occurs at high crack tip strain rates ($=10^{-2}$ s^{-1}), where the environmental crack growth rate saturates because a bare surface is maintained continuously at the crack tip (i.e. equation 4). Another limit occurs at low crack tip strain rates due to crack blunting (i.e. when the corrosion rate of the crack sides approaches the oxidation rate at the crack tip).

The model has been quantified by evaluating the following processes: (1) the steady state and transient compositions of the environment at the crack tip as a function of the conditions in the bulk (external) solution; (2) the oxidation rates for the material/environment system expected at a strained crack tip; and (3) the oxide fracture strain and the crack tip strain rate, defined in terms of engineering parameters such as K,

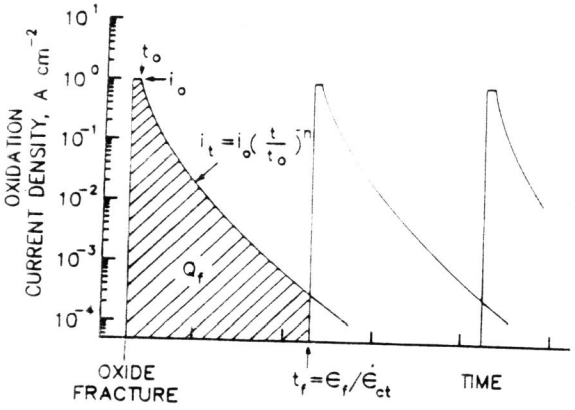

$$V = \frac{dq}{dt} \; ; \; \bar{V}_{av} = \frac{M}{z\zeta F} \cdot \frac{Q_f}{t_f}$$

FOR HIGH $\dot{\epsilon}_{ct}$ AND/OR LONG t_o :

$$\bar{V}_{av} = \frac{M}{z\zeta F} \cdot i_o$$

FOR LOW $\dot{\epsilon}_{ct}$ AND/OR SHORT t_o :

$$\bar{V}_{av} = \frac{M}{z\zeta F} \frac{i_o t_o^n}{(1-n)\epsilon_f^n} \dot{\epsilon}_{ct}^n = f(n)\, \dot{\epsilon}_{ct}^n$$

Figure 4 Oxidation current density/time transients at a crack tip which is subjected to a strain rate, $\dot{\epsilon}_{ct}$.

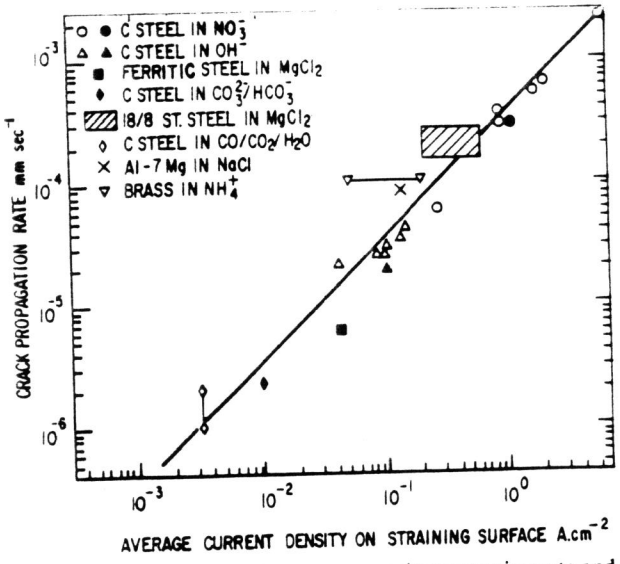

Figure 5 Relationship between the average crack propagation rate and the oxidation kinetics on a straining surface for several ductile alloy/aqueous environment systems. (9,33)

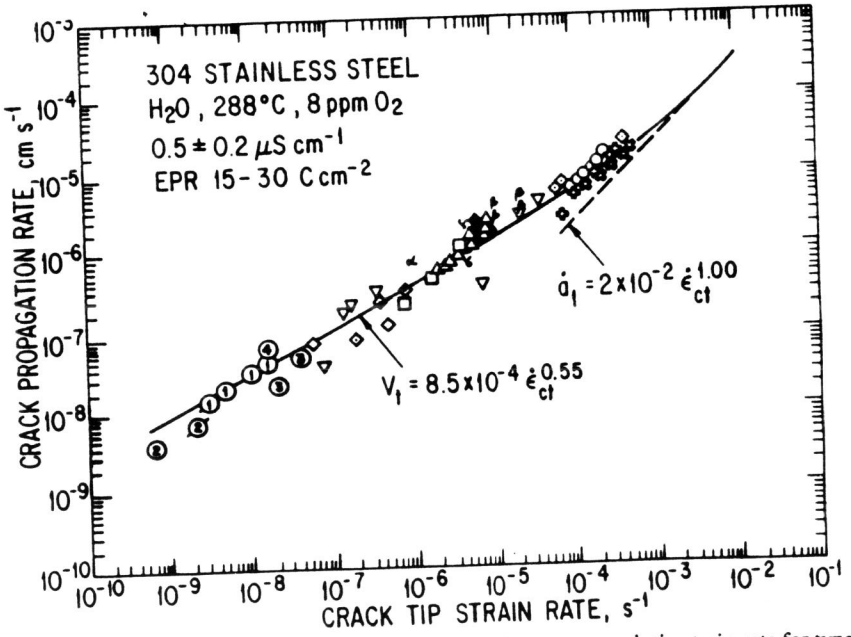

Figure 6 Observed and predicted crack growth rate vs. crack tip strain rate for type 304 stainless steel. The film rupture model predicts a maximum in crack velocity at crack tip high strain rates associated with the bare surface dissolution rate. The dotted line shows the contribution of the inert fatigue crack growth rate. (30)

ΔK, R, frequency, etc. These tasks have been discussed in detail elsewhere for stainless steels (30,34-36), low alloy and carbon steels (30, 34, 35, 37-40), ductile nickel alloys (34-36,41-43) and irradiated stainless steels (35,44-47). Additionally, short crack behavior and the transition to long crack behavior(48,49), concerns for crack chemistry similitude (16,17), treatment of thickness and time-varying properties, and treatment of distributions in properties and statistical approaches (33, 34, 35, 38-40) have also been addressed. This paper will illustrate the validity and practical use of a prediction model based on Equation 5 .

EVALUATION OF CRACK GROWTH RATE PREDICTIONS

Observed crack growth rates for various combinations of stainless steel microstructure, dissolved oxygen content, solution purity and stressing mode have been compared with the values predicted by the slip dissolution/film rupture model via Equation 5. The correlation between observed and predicted crack velocity/strain rate relationships is shown in Figure 6 for furnace sensitized type 304 stainless steel in aerated water at 288°C under static, monotonically increasing, and cyclic loading conditions.

It is assumed that under fatigue loading the crack advance mechanisms due to slip-dissolution and striation/micro void coalescence (associated with "dry" fatigue processes) are independent; thus the amount of crack advance under corrosion-fatigue situations is given by the superposition or addition of these two components. Therefore, two factors are noteworthy in Figure 6; first, the extent of environmentally-assisted crack advance is correctly predicted for a wide range of stressing conditions, where the crack tip strain rate is the normalizing parameter and, second, the crack propagation rate at the high crack tip strain rates possible under certain fatigue loading conditions is dominated by the dry-fatigue mechanism.

Similar agreement between observation and theory is obtained for other environmental conditions associated, e.g., with the synergistic effects of corrosion potential (e.g. dissolved oxygen and radiation flux) and solution conductivity (or anionic activity) (Figure 7). The overall agreement between observation and prediction for the stainless steel/water system is illustrated in Figure 8 as the ratio (predicted/observed) of the crack growth rates over a wide rage of material, environment, and loading conditions. The mean value of this ratio is 1.17, and the variance in the distribution can be correlated with the uncertainty in the system definition (33,34-36). Similar predictive accuracy has been obtained for low alloy steels (33,34,35, 38-40), ductile nickel alloys (34, 35, 41-43), and irradiated stainless steel (44-47).

APPLICATIONS OF PREDICTIVE MODELING

The ability to predict environmentally assisted crack growth rates in high temperature water with reasonable accuracy has considerable practical impact. For example, it provides a methodology for evaluating the quantitative benefit and overall validity of empirically derived remedies that have often been based on accelerated test data. Also, it provides the ability to optimize inspection intervals and plant operating conditions with regard to resistance to environmental cracking. Finally, it provides a basis for improved design and lifetime evaluation codes, as well as plant life extension decisions.

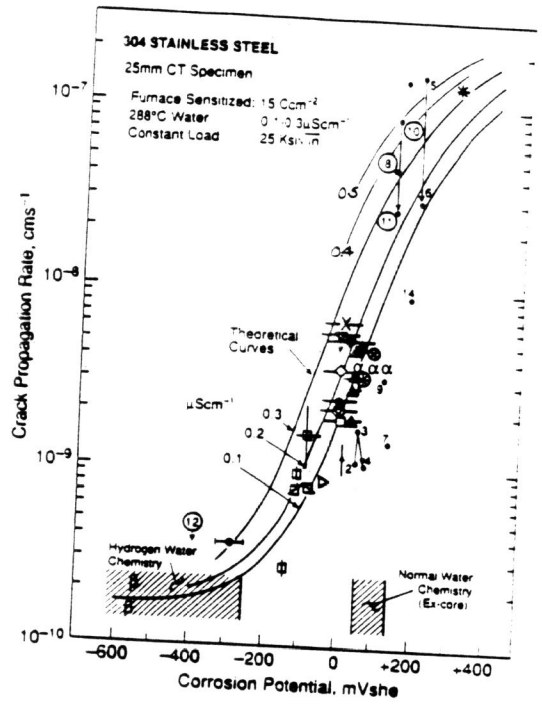

Figure 7 **Comparison of observed vs. predicted crack growth rate as a function of corrosion potential for sensitized type 304 stainless steel at constant load. Data points at elevated corrosion potentials and growth rates correspond to irradiated water chemistry conditions in test or commercial reactors (33,34-36)**

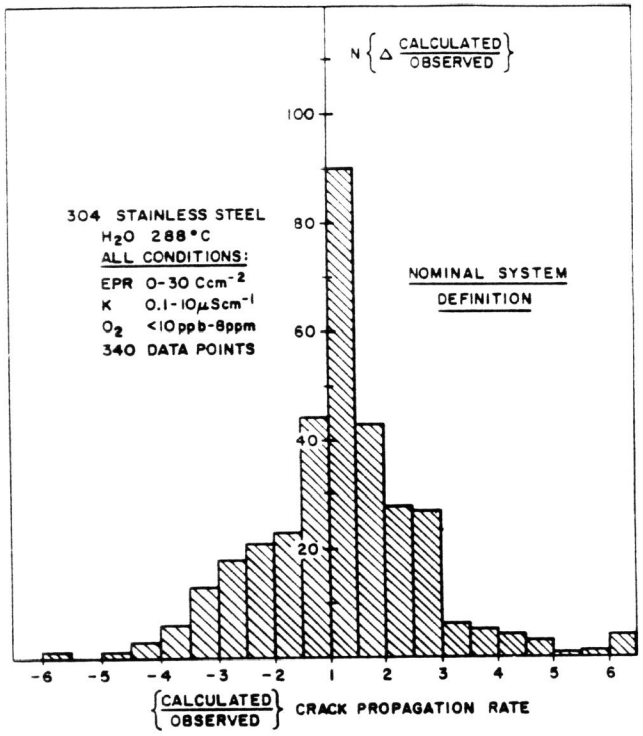

Figure 8 Frequency distribution of the ratio of the calculated-to-observed crack growth rate for type 304 stainless steel in 288°C water (33,34-36).

Examination of the validity of the current ASME XI (1980) lifetime evaluation codes for low alloy steel pressure vessels and piping undergoing corrosion fatigue indicates that the maximum predicted (da/dn) vs. ΔK values approximate those in that evaluation code, Figure 9[56]. It is also apparent, however, that the use of the cyclic based code can be conservative, especially for the majority of the stressing, material, and environmental conditions shown in Figure 9. Under these corrosion fatigue conditions and, clearly, static loading conditions, it is more appropriate to use a time based code (50).

A similar evaluation was undertaken for stainless steels in high temperature water, whereby a family of curves were developed to reflect actual differences in plant operating conditions. Rather than relying on a single evaluation curve (e.g., the NRC disposition curve (51) (Figure 10a), this approach eliminates unnecessary conservatism by providing plant-and-condition-specific predictions (Figures 10, b, c). Similarly, informed operational decisions can be made to permit, e.g., appropriate control of corrosion potential, conductivity, and other inter-related parameters to ensure satisfactory stress corrosion resistance.

With respect to the empirically derived remedies for sensitized stainless steel piping in BWR's, it was verified (33,34-36) that reducing the tensile (especially weld residual) stress, decreasing the corrosion potential (e.g., by hydrogen addition into the feed water), solution conductivity, or the grain boundary sensitization should decrease the crack growth rate to the extent observed in qualification tests performed by the reactor manufacturers and confirmed by other laboratories. Moreover, the modeling predicts the observed variation in cracking susceptibility of piping with, e.g., conductivity, and can identify the combinations of corrosion potential and conductivity that must be achieved to ensure satisfactory stress corrosion resistance.

Integration of an expanded version of equation 2 and inserting a derived algorithm for the crack tip strain rate as a function of the stress intensity, K,

$$\dot{\varepsilon}_{ct} = CK^4 = C\pi^2 a^2 (B\sigma)^4 \qquad [6]$$

leads to a quantitative version of the schematic crack depth/time curves shown in Figure 1;

$$a_t = \left\{ a_i^{(1-2n)} + 7.8\times10^{-3} n^{3.6} (1-2n)[C\pi^2 a^2 (B\sigma)^4]^n . t \right\}^{1/1-2n} \qquad [7]$$

In this equation a parameter a_i is needed since the formulation of equation 6 was originally validated for precracked fracture-mechanics type specimens, and the concept of an "intrinsic" defect a_i was needed for applications to an initially undefected surface. In numerous applications of the model to smooth stainless steel components a value of a_i = 50 μm as proven satisfactory.

The use of equation 7, in conjunction with the variation in stress intensity with varying residual stress adjacent to welds leads to the prediction of the effects of, for

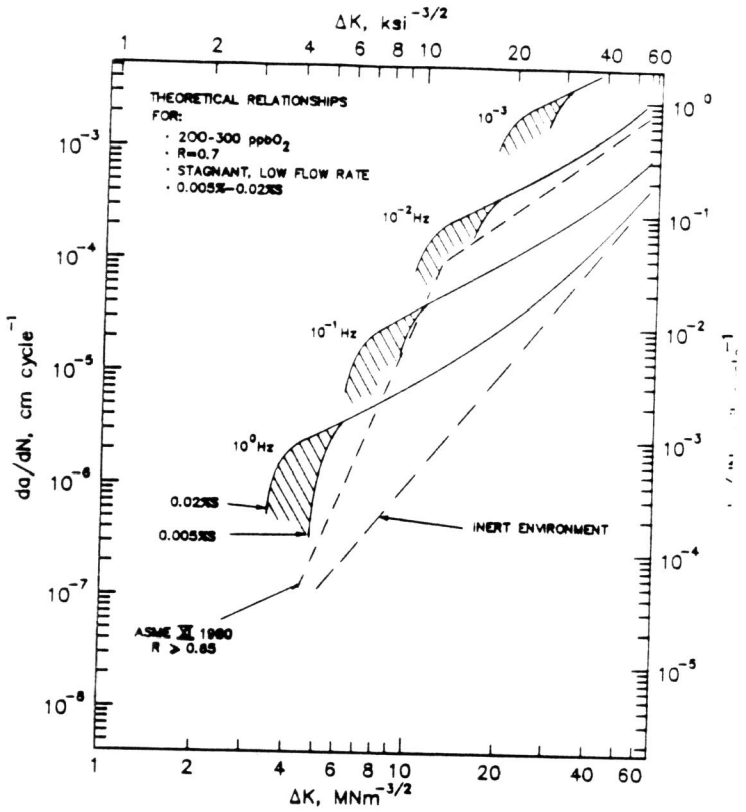

Figure 9 Predicted da/dN vs. ΔK relationships for A533B/A508 pressure vessel steel cyclically loaded at various frequencies under R=0.7 conditions. (39)

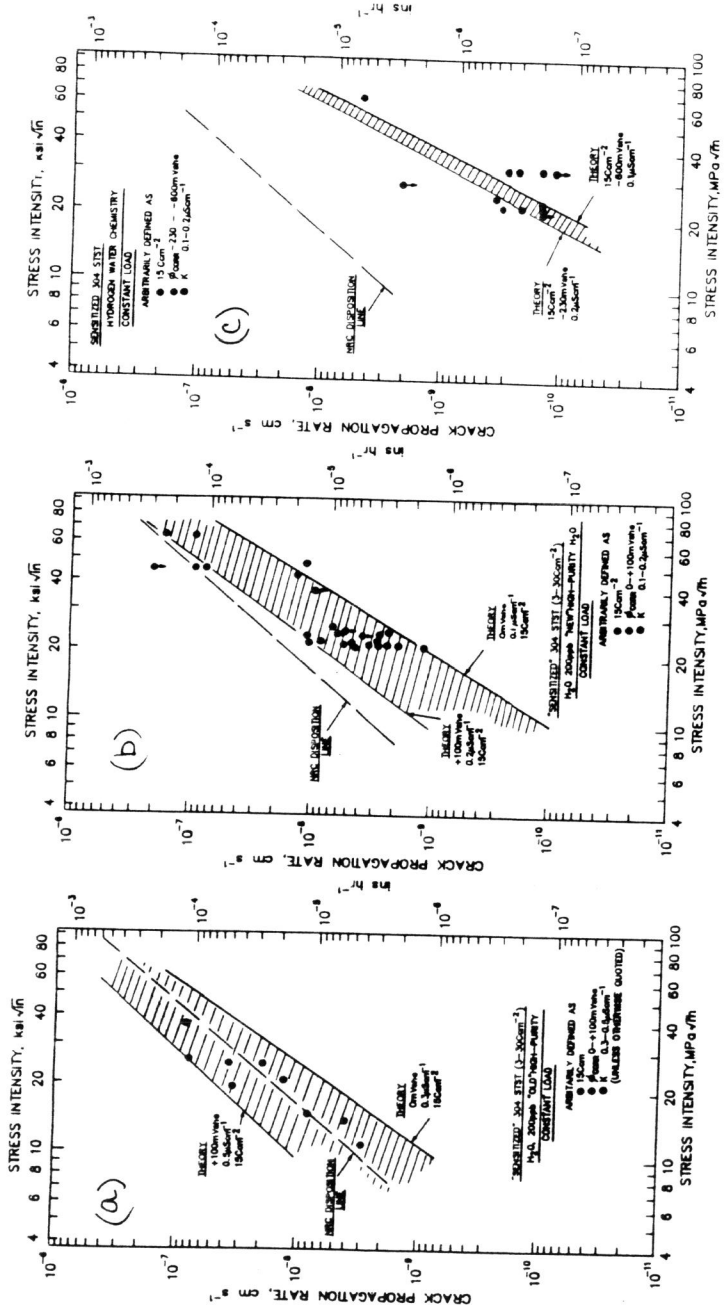

Figure 10 Relationship between the empirically derived NRC disposition line (19) for sensitized type 304 stainless steel in 200 ppb oxygenated water with 0.4 ± 0.1 μS cm^{-1} purity at 288°C and (a) the predicted band for this defined water chemistry. In Figures 10b and 10c are shown the observed and predicted crack propagation rate/stress intensity relationships for (b) improved water purity 0.15± 0.05 μScm^{-1} and (c) deaerated high purity water.

instance, changing the solution purity on the crack depth/operating time for stainless steel piping, and the range of crack depths within a given plant piping system due to the range in residual stress in the HAZ adjacent to a weld (Fig. 11). Such a range of actual system conditions automatically leads to a predictable range in observed cracking response in the operating plant; this is illustrated in Figure 12 for the theoretical relationships between the operating time required for a crack to penetrate a quarter wall thickness in a welded 304 stainless steel pipe and the coolant purity. These theoretical relationships are shown for a range of carbon contents (i.e. EPR values), and residual stress profiles; it is seen that the observed data lie between the theoretical bounds. Thus, with this proven prediction capability, quantitative decisions may be made about the future behavior of plant for proposed material, stress or environmental modifications (Figure 13).

The behavior of ductile nickel base alloy components has also been evaluated. Comparatively extensive statistical data on environmental cracking of Inconel 600 shroud head bolts (43) were obtained in the form of the incidence of cracking (percentage of cracked bolts normalized by plant operating time). Modeling predictions are in reasonable agreement with these observations (Figure 14).

Modeling extensions to permit predictions of irradiation assisted stress corrosion cracking (IASCC) have also been performed (44-47). Of primary importance are the effects of radiation on water chemistry (in elevating the corrosion potential), the effects of radiation induced segregation (in causing depletion and enrichment of elements at the grain boundary), and the effects of radiation creep on stress relaxation. These extensions were quantified using data from a variety of sources including, e.g., in-situ measurements of corrosion potential and crack growth rates in the core of commercial BWRs (Figures 7 and 15) (44, 45, 52). Reasonable predictions of IASCC data from irradiated specimens (44-47, 53) of stainless steel (Figures 15 and 16) and IASCC cracking incidence in a variety of core internals (Figure 17) were obtained (44-47), thereby providing the basis for plant life extension decisions.

CONCLUSIONS

1. The slip dissolution/film rupture model for environmentally assisted crack growth is capable of predicting the observed crack growth rates for the stainless steels, nickel alloys, and low alloy steels in high temperature water systems over a wide range of material, environment, loading, and irradiation conditions. The accuracy of the prediction is strongly dependent on detailed knowledge of the system conditions. This is optimally achieved by integrating the predictive capabilities with system monitors.

2. The mechanism correctly predicts the effect on the crack growth rate of stressing parameters, spanning constant load, monotonically increasing load, and cyclic load over a wide range load of amplitudes, mean load, and frequency conditions, as reflected in the crack tip strain rate.

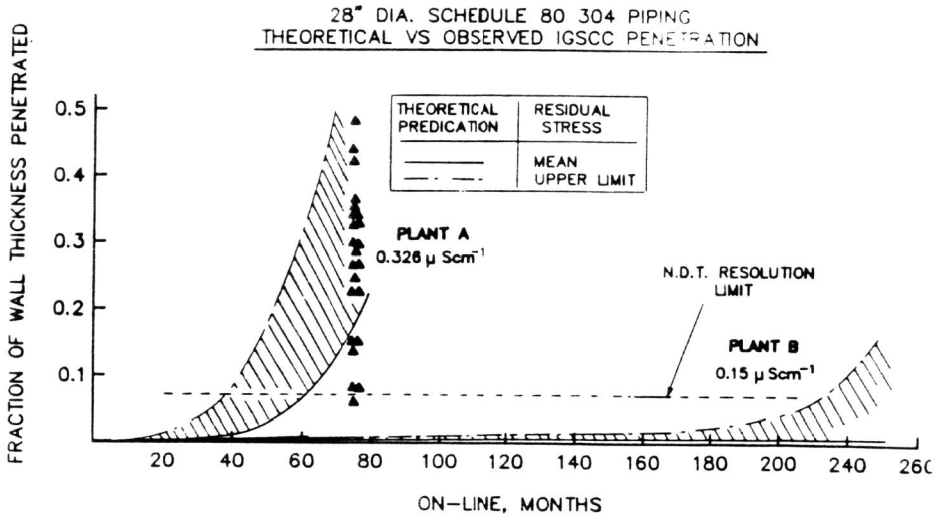

Figure 11 Theoretical and observed cracked depth v. operational time relationships for 28" diameter Schedule 80 304 stainless steel piping for two Boiling Water Reactors operating at different mean coolant conductivities. Note the bracketing of the maximum crack depth in the lower purity plant by the predicted curve that is based on the maximum residual stress profile, and the predicted absence of observable cracking in the higher purity plant (in 240 operating months).

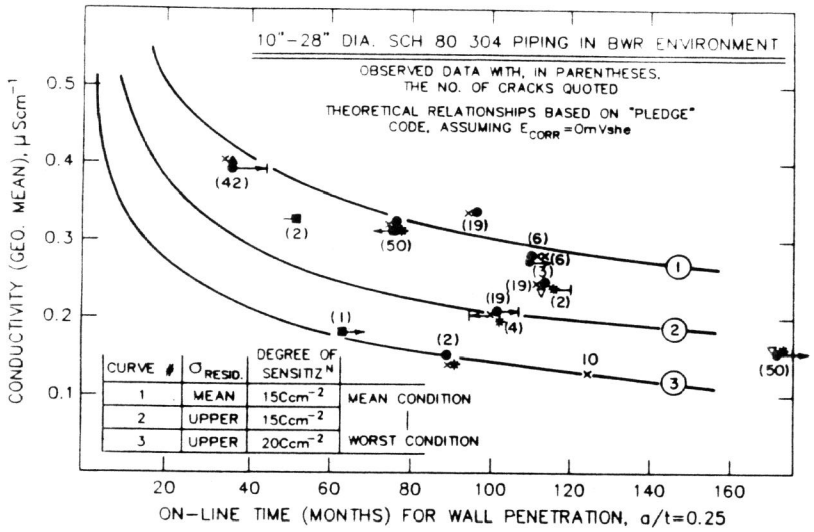

Figure 12 Observed and predicted relationships between average BWR coolant conductivity and the operational time to achieve quarter wall penetration. Observed data from various operational BWR's and pipe diameters are shown with the number of cracks observed at each data point shown in parenthesis. Predicted curves are for the quoted combinations of stress and degree of sensitization at the HAZ.

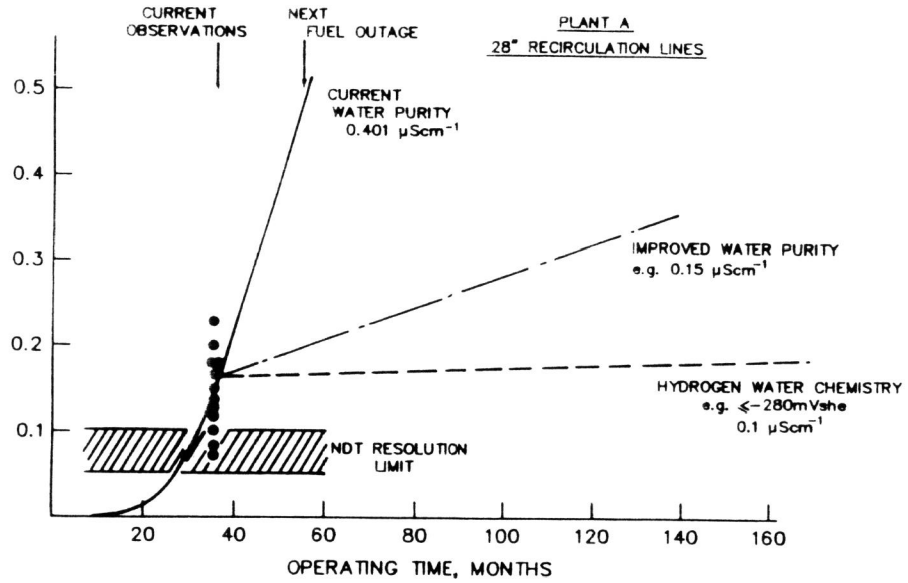

Figure 13 Predicted response of defected piping for defined changes in water chemistry in BWR plant.

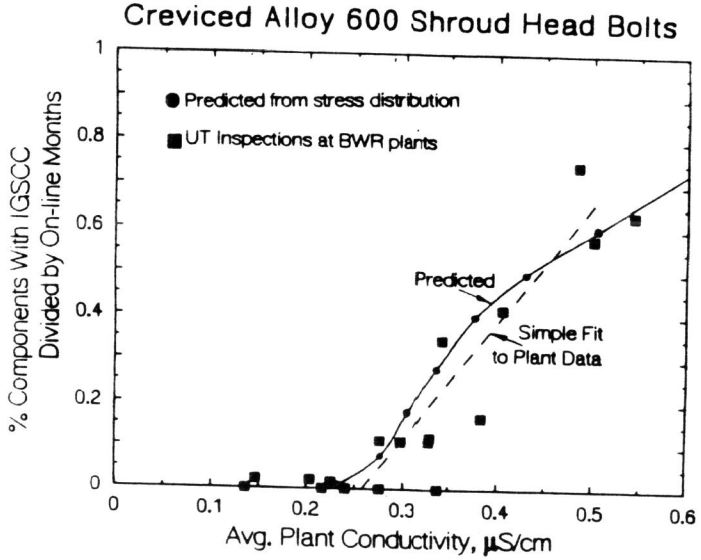

Figure 14 Predicted and observed effect of solution conductivity on statistics of cracking incidence in shroud head bolts, expressed as the percentage of the components which were inspected which possessed detectable cracks, normalized by the on-line exposure time.

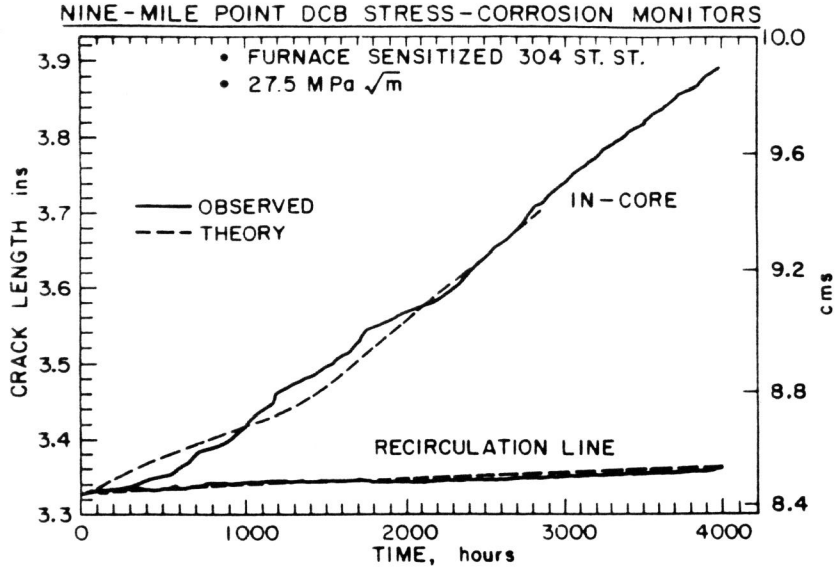

Figure 15 Predicted and observed crack depth/time relationships for furnace-sensitized type 304 stainless steel DCB specimens exposed in the reactor core or in the unirradiated recirculation line at Nine-Mile Point BWR. The difference in the propagation rates is predictably due to the measured differences in corrosion potential at these two locations.

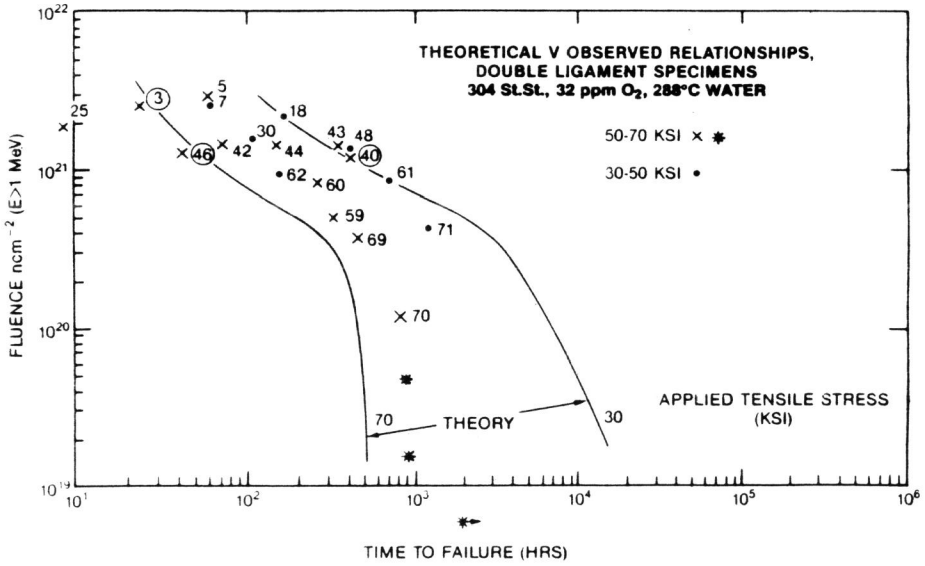

Figure 16 Comparison between observed (53) and predicted (45-47) time-to-failure for the effect of fast neutron fluence on pre-irradiated type 304 stainless steel tested at constant load in the laboratory in oxygen saturated, 288°C water.

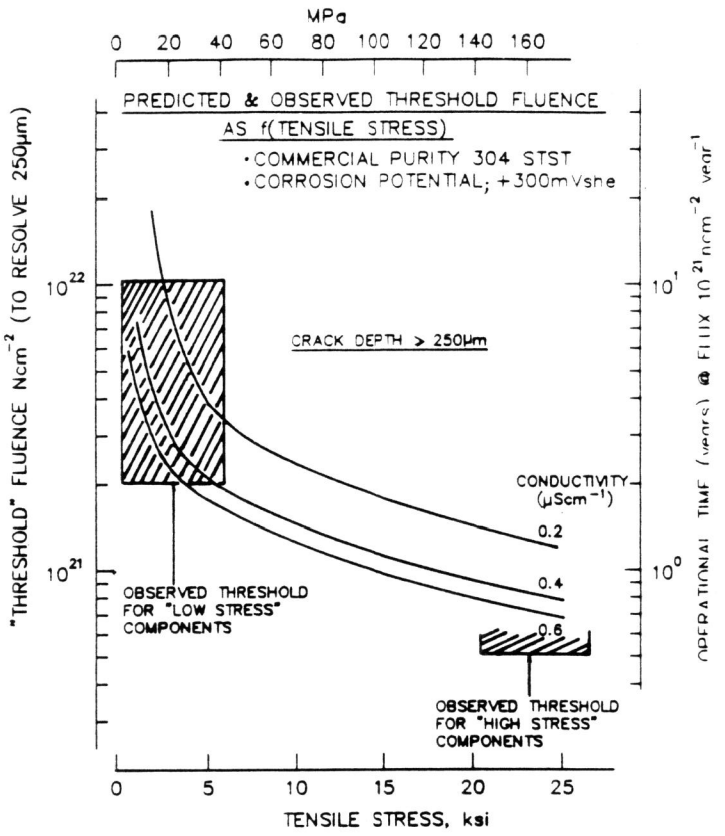

Figure 17 Predicted threshold fluence vs. solution conductivity for type 304 stainless steel reactor internals components. Curves are shown for various stress levels along with observed threshold fluences for "high" and "low" stress core components in operating BWR's (44-47). Predictions involve stress intensity vs. crack depth/time calculations which account for the complex variation in residual stress vs. wall thickness with relaxation vs. time from neutron irradiation.

3. This approach provides theoretical underpinning to the empirically derived remedies for intergranular and irradiation assisted stress corrosion cracking of stainless steels and nickel alloys, and confirms that, for extended time periods, the ASME XI (1980) lifetime evaluation code for corrosion fatigue of low alloy pressure vessel steels is probably conservative.

REFERENCES

1. S. Suresh and R. Ritchie, "The Propagation of Short Fatigue Cracks", U. of California. Berkeley Report UCB/RP/83/1014, June 1983.
2. J. Lankford, Fatigue Engineering Materials and Structures 6, 15, 1983.
3. S. Pearson, Engineering Fracture Mechanics 7, 235, 1975.
4. W.L. Morris, O. Buck and H.L. Marcus, met. Trans. A74, 1161, 1976.
5. M.H. El Haddad, T.H. Topper and B. Mukherjee, J. Test Eval. 9, 65, 1981.
6. R.N. Parkins, Corrosion 43, 130, 1987.
7. R.N. Parkins and P.M. Singh, Corrosion, 46, 485-498, 1990.
8. P.L. Andresen, I.P. Vasatis and F.P. Ford, "Behavior of Short Cracks in Stainless Steel at 288°C", Paper 495, NACE Conference, Las Vegas, April 1990.
9. F.P. Ford, "Mechanisms of Environmental Cracking Peculiar to the Power Generation Industry", Report NP2589, EPRI, Palo Alto, September 1982.
10. F.P. Ford, "Stress Corrosion Cracking", in Corrosion Processes, Ed. R.N. Parkins, Applied Science, 1982.
11. R.N. Parkins, N.J. H. Holroyd and R.R. Fessler, Corrosion 34, 253, 1978/
12. T.P. Hoar and G.P. Rothwell, Electrochem, Acta 15, 1037, 1976.
13. T.R. Beck, Corrosion 30, 408, 1974.
14. C. Manfredi, I. Maier and J.R. Galvale, Corr. Sci. 27, 887, 1987.
15. J.M. Sutcliffe, R.R. Fessler, W.K. Boyd and R.N. Parkins, Corrosion 28, 313, 1972.
16. B. Poulson and R. Robinson, Corr. Sci. 20, 707, 1980.
17. J. Congleton, "Some Aspects of Crack Initiation in Stress Corrosion and Corrosion Fatigue", Corrosion-88, St. Louis, March 21-25, 1988.
18. "Environmental-Sensitive Mechanical Behavior", Baltimore, Maryland, June 1965. (ARC Westwood and N.S. Stoloff, Ed.), Gordon and Branch.
19. "Fundamental Aspects of Stress-Corrosion Cracking", Ohio State University, September 1967, (R.W. Staehle, A.J. Forty and D. VanRooyen, Ed.), NACE, Houston.

20. "Theory of Stress Corrosion Cracking", Ericera, Portugal, March, 1971, (J.C. Scully, Ed., Pub. NATO Brussels).

21. "Corrosion Fatigue Chemistry, Mechanics and Microstructure", University of Connecticut, Storrs, June, 1971. (O. Devereaux, A.J. McEvily and R.W. Staehle, Ed.), NACE, Houston, 1972.

22. "L'Hydrogene dans les Metaux", Paris, 1972. (M.P. Bastein, Ed.), Science et Industrie.

23. "Hydrogen in Metals, L" (I.M. Bernstein and A.W. Thompson, Ed.), ASM, 1973.

24. "Stress-Corrosion Cracking and Hydrogen Embrittlement of Iron-Base Alloys", Firminy, France, June 1973. (R.W. Staehle, J. Hochmann, R.D. McCright and J.E. Slater, Eds.), NACE, Houston, 1977.

25. "Effect of Hydrogen on Behavior of Materials", Jackson Lake, Wyoming, September 1975. (A.W. Thompson and I.M. Bernstein, Ed.), AIME.

26. "Surface Effects on Crystal Plasticity, Hohegeiss, Germany, September 1975. (R.M. Latanision and J.T. Fourie, Ed.), Noordhof-Leyden, 1977.

27. "Mechanisms of Environment Sensitive Cracking of Materials", University of Surrey, United Kingdom, April 1977. (P.R. Swann, F.P. Ford and A.R.C. Westwod, Ed.), The Metals Society.

28. "Corrosion-Fatigue", University of Newcastle, April 1979, Met. Sci. 13, 1979.

29. R.N. Parkins, British Corr. J. 7, 15, 1972.

30. F.P. Ford, D.F. Taylor, P.L. Andresen and R.G. Ballinger, "Corrosion-Assisted Cracking of Stainless Steel & Low-Alloy Steels in LWR Environments", Report NP5064-S, February 1987, EPRI, Palo Alto.

31. R.N. Parkins and B.S. Greenwell, Met. Sci. 405, August 1977.

32. C. Laird and D.J. Duquette, as Ref. 26, p. 88.

33. R.N. Parkins, "Environment-Sensitive Fracture-Controlling Parameters", Proceedings of 3rd International Conf. on Mechanical Behavior of Materials, Cambridge 1979, (Ed.) K.J. Miller, R.F. Smith, (Pub.) Elsevier, N.Y., Vol. 1, pp. 139-164.

34. F.P. Ford and P.L. Andresen, "Development and Use of Predictive Model of Crack Propagation in 304/316L, A533B/A508 and Inconel 600/182 in 288°C Water", 3rd Int.Conf. on Degradation of Materials in Nuclear Power Industry, TMS-AIME, pp. 789-800, 1988.

35. P.L. Andresen and F.P. Ford, "Life Prediction by Mechanistic Modeling and System Monitoring of Environmental Cracking of Fe and Ni Alloys in Aqueous Systems", Materials Science and Engineering, A103, pp. 167-183, 1988.

36. F.P. Ford, P.L. Andresen, H.D. Solomon, G.M. Gordon, S. Ranganath, D. Weinstein, and R. Pathania, "Application of Water Chemistry Control, On-Line Monitoring and Crack Growth Rate Models for Improved BWR Materials Performance", Proc. Fourth Int. Symp. on Environmental Degradation of Materials in Nuclear Power Systems - Water Reactors, NACE, pp. 4-26 to 4-51, 1990.

37. F.P. Ford and P.. Emigh, Corr Sci 2, 8/9, 673-692, 1985.

38. F.P. Ford, P.L. Andresen, D. Weinstein & S. Ranganath, "Stress Corrosion Cracking of Low Alloy Steels in High Temperature Water", Proc. Fifth Int. Symp. on Environmental Degradation of Materials in Nuclear Power Systems-Water Reactors, ANS, 1991.

39. F.P. Ford and P.L. Andresen, "Corrosion Fatigue of A533B/A508 Pressure Vessel Steels in Water at 288°C," Proc. Third Intl. Atomic Energy Agency Specialists Mtg on Subcritical Crack Growth, Moscow, USSR, May 1990, NRCNUREG/CP-0112 (ANL-90/22), Vol. 1, p. 105-124.

40. F.P. Ford and P.L. Andresen, "Stress Corrosion Cracking of A533B/Pressure Vessel Steels in Water at 288°C", Proc. Third Intl. Atomic Energy Agency Specialists Mtg. on Subcritical Crack Growth, Moscow, USSR, May 1990, NRC NUREG/CP-0112 (ANL-90/22), Vol. 2, p. 37-54.

41. P.L. Andresen, "Fracture Mechanics Data and Modeling of Environmental Cracking of Nickel-Base Alloys in High Temperature Water", Paper #44, Corrosion/91, NACE, Houston, March 1991.

42. P.L. Andresen, "Development of Data and Predictive Models for Environmental Cracking of Nickel Alloys in 288°C Water", Final Report on EPRI Contract RP2006-17, May 1991.

43. K.S. Brown, P.L. Andresen and G.M. Gordon, "Modeling of Creviced Alloy 600 Shroud Head Bolt SCC Field Experience", Proc. Life Prediction of Corrodible Structures, Hawaii, November 1991, NACE.

44. P.L. Andresen, F.P. Ford, S.M. Murphy, J.M. Perks, "State of Knowledge of Radiation Effects on Environmental Cracking in Light Water Reactor Core Materials", Invited Review Paper, Proc. Fourth International Symposium on Environmental Degradation of Materials in Nuclear Power Systems, Jekyll Island, GA, August 1989, NACE, 1990, pp. 1-83 to 1-121, 1990.

45. P.L. Andresen, "Irradiation Assisted Stress Corrosion Cracking", in Book on Stress Corrosion Cracking, July 1991, Ed. R. Jones, ASM, to be published, March 1992.

46. F.P. Ford and P.L. Andresen, "Lifetime Prediction of Irradiation Assisted Stress Corrosion Cracking in 288°C Water. Part II: Application of Modeling to Laboratory and Field Data", Proc. Life Prediction of Corrodible Structures, Cambridge, September 1991, NACE.

47. F.P. Ford and P.L. Andresen, "Lifetime Prediction of Irradiation Assisted Stress Corrosion Cracking in 288°C Water, Part II: Application of Modeling to Laboratory and Field Data", Proc. Life Prediction of Corrodible Structures, Cambridge, September 1991, NACE.

48. Peter L. Andresen, Ioannis P. Vasatis & F. Peter Ford, "Behavior of Short Cracks in Stainless Steel at 288°C", Paper #495, Corrosion/90, Las Vegas, 1990, NACE, Houston.

49. Peter L. Andresen and F. Peter Ford, "Measurements, Relationships and Application of Short Crack Growth Rates to Lifetime Prediction", Proc. Life Prediction of Corrodible Structures, Hawaii, November 1991, NACE.

50. J.D. Gilman, "Application of a Model for Predicting Corrosion Fatigue Crack Growth in Reactor Pressure Vessels in LWR Environments", Proc. ASME Symp on "Predictive Capabilities in Env Assisted Cracking", Miami, Nov. 1985, pp. 1-16.

51. W.S. Hazelton, "Technical Report on Material Selection and Processing Guidelines for BWR Coolant Pressure Boundary Piping", Draft Report NUREG0313, Rev. 2, U.S. Nuclear Regulatory Commission.

52. R.A. Head, M.E. Indig and P.L. Andresen, "Measurement of In-core and Recirculation System Responses to Hydrogen Water Chemistry at Nine Mile Point Unit 1 BWR", EPRI Contract RP2680-5, Final Report, 1989.

53. A.J. Jacobs and G. P. Wozadlo, "Stress Corrosion Testing of Irradiated Type-304 Stainless Steel Under Constant Load", Paper #41, Corrosion/91, Cincinnati, NACE, Houston, 1991.